J Electroceram (2006) 16: 41–47
DOI 10.1007/s10832-006-2366-8

Corrosion performance of lamellae nanostructured fluorinated organic coating applied on steel

V. Roche · F. Vacandio · D. Bertin · Y. Massiani

Received: January 27, 2005 / Revised: April 27, 2005 / Accepted: May 18, 2005

Abstract This work investigates a new organic coating for corrosion protection. This coating is a Poly(*n*-butyl acrylate-*b*-trifluoroethyl methacrylate) diblock copolymer elaborated by Controlled Radical Polymerization and then deposited on steel. Several parameters were taken into account to evaluate their influence on corrosion protection properties: the PBA molar mass, the solvent type (THF or Dichloromethane), the thickness of coatings and the nature of the nanostructuration (lamellae or sphere). The thickness of the films was measured between 45 and 265 μm by optical microscopy and by gravimetric difference measurements. Atomic Force Microscopy (AFM) observations show a homogeneous surface of the coating with a nanostructured lamellar structure. The electrochemical behaviour was studied by Electrochemical Impedance Spectroscopy (EIS) in a sodium sulphate solution. The better corrosion resistance was obtained for coating thickness higher than 265 μm. On the other hand, poor results were obtained using a PBA high molar mass and dichloromethane as solvent.

Keywords Diblock copolymers · Controlled radical polymerisation · Nanostructuration · Corrosion · Electrochemical characterisation

V. Roche · F. Vacandio (✉)· Y. Massiani
Laboratoire MADIREL, UMR 6121 CNRS-Université de Provence, Centre Saint-Jérôme 13397 Marseille, Cedex 20, France
e-mail: vacandio@up.univ-mrs.fr

V. Roche · D. Bertin (✉)
Laboratoire CBRL, UMR 6517 CNRS-Universités d'Aix-Marseille I et III, Centre de Saint-Jérôme 13397, Marseille Cedex 20, France
e-mail: denis.bertin@up.univ-mrs.fr

1. Introduction

The annual production of steel is 170 million tons. On this tonnage, it is estimated that the corrosion degrades 50 millions tons. Consequently, new processes for corrosion protection are constantly in progress to stop this degradation. At present, the protection by organic coatings and more exactly by systems of paintings is very trendy. These paintings are usually formulated from five constituents [1–4]: (a) Main constituent is the binder matrix (polymer) which gives the main properties to the coating such as corrosion protection (usual binders are epoxy, polyurethane, alkyde...). (b) Pigments: inorganic (essentially for corrosion protection) or metallic. (c) Extenders to reduce the economic cost. (d) Additives for specific properties: anti-foamers, fire retarding agents, anti-coalescence agents, UV-absorbers... (e) The components are dissolved in a solvent before application, to reduce the viscosity of the coating and to control the drying. Reduction of viscosity is also necessary for a good dispersion of pigments in the binder matrix.

The majority of coatings for corrosion protection are multilayers systems:

(1) the "primer" layer (with a thickness of about 20 to 50 μm) directly in contact with the substrate (must have a good adhesion to the substrate and good corrosion protection properties).
(2) some intermediate layers (100 to 150 μm) to make a barrier to penetration of aggressive substances.
(3) and finally the last layer called "top coat" (about 50 μm) directly exposed to the environment which gives the final visual aspect (coloration...) and must resist to exterior aggressions.

Our objective was, instead of having a complete system, to obtain a binder including all the properties of a complete

system applicable in a single layer. To reach this objective, the idea was to combine various properties of polymers (adhesion, low water permeability, UV resistance) using a diblock copolymer as a monocomponent system. In a diblock copolymer, one chain portion is attached to another, end to end [5]. Thus, the presence of the chemical bond between the blocks definitely improves the mutual miscibility of the two polymers. Then a nanoscale self-organization of such copolymers can be easily achieved. Various nanostructures could be obtained from sphere, cylinder, bicontinuous to lamellae organization, governed mainly by the composition of the diblock copolymer [6]. To improve adhesion on steel, a Poly(*n*-butyle acrylate) (PBA) block was chosen for its amorphous and elastomer properties. The second block was a fluorinated polymer as Poly(trifluoroethyl methacrylate) (PTFEMA), which was chosen for its rigidity and good water impermeability (due to the presence of fluorine atoms). A preferred way of synthesis was selected based on radical polymerization for the diblock copolymers preparation. Using nitroxyde in the radical polymerization mixture, the livingness and the control are achieved, similar to ionic polymerization keeping the advantages of radical polymerization [7]. Symmetric block copolymers (PBA-b-PTFEMA) were targeted for corrosion protection due to their ability to organize in multilayered lamellae nanostructure forming a good barrier against corrosive substances.

In this study, after having estimated the thickness of the coatings, the first stage was to examine their structure by Atomic Force Microscopy (AFM) in order to verify the expected lamellae nanostructure. The coatings were then characterised by Electrochemical Impedance Spectroscopy (EIS) to evaluate their corrosion protection properties. EIS is the most often used method to investigate the corrosion resistance of an organic coating [1, 8–11]. From the diagrams obtained, it is possible to model the behaviour of the coating deposited on a substrate using equivalent electrical circuits [8] and then to estimate numerous parameters such as the interfacial capacitance of the coating [8, 9], the fraction of absorbed water [8, 10, 11] which reflects the presence of defects, the reactivity of the interface, the adhesion and the barrier properties to water.

2. Experimental

2.1. Synthesis of the copolymers

The Poly(*n*-butyl acrylate-*b*-trifluoroethyl methacrylate) copolymer was elaborated by controlled radical polymerisation in the presence of nitroxyl radicals. *n*-butyl acrylate monomer (BA) (Fig. 1(a)), MAMA-SG1 alcoxyamine (Fig. 1(b)) and free SG1 (Fig. 1(c)) were charged in a glass reactor provided with a cooler, with an inflow of sluggish gas (N_2). Three Poly(*n*-butyl acrylate) (PBA) blocks (Fig. 1(d)) were synthesised. The medium of polymerization is degassed by nitrogen bubbling during 20 min and placed under magnetic stirring in a thermostated oil bath by realizing a thermal ramp up to 120°C. The quantities of every reagent as well as the reaction times are presented in Table 1. After end of the synthesis, residual monomer is eliminated by stripping under reduced pressure.

Then these Poly(*n*-butyl acrylate) blocks were used as macro–initiator to synthesise the Poly(trifluoroethyl methacrylate) (PTFEMA) blocks. The procedure is similar,

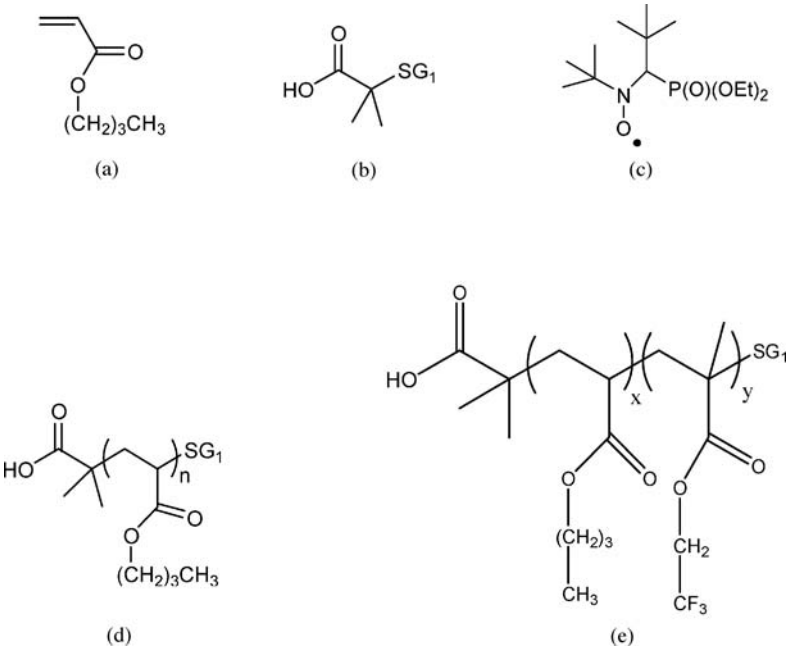

Fig. 1 (a) *n*-butyl acrylate monomer, (b) MAMA-SG1 alcoxyamine, (c) Free SG1, (d) Poly(*n*-butyl acrylate) (PBA) block, (e) Diblock copolymer Poly(*n*-butyl acrylate-*b*-trifluoroethyl methacrylate)

except that the temperature is 90–100°C. The quantities of every reagent as well as the reaction times are summarized in the Table 2. Once the ended synthesis, staying monomer is eliminated by stripping under reduced pressure. The diblock copolymer obtained is presented on Fig. 1(e).

2.2. Elaboration of coatings

The films were deposited in two steps: dissolution of the copolymer in a solvent, deposition of the solution obtained ($C = 6.4 \times 10^{-3}$ mol·L^{-1}) on the steel substrate and evaporation of the solvent. The substrates are low carbon steel panels (A366 ASTM type) (6.5 cm × 6.5 cm). Before coating, these panels were cleaned in ethanol using an ultrasonic rinse and then dried under compressed air. The samples obtained are summarized in Table 3. Three parameters vary: first the type of solvent used, Tetrahydrofuran (THF) or dichloromethane, second, the average molecular mass of the PBA block and third, the thickness of the coating through the number of identical layers (one, three or six) deposited on the substrate.

2.3. Thickness of films

The thickness of the organic coatings was estimated using two different methods: by mass difference measurements of the substrate before and after organic coating deposition using a Mettler Toledo balance (PG5002-S, 0.1 mg for the precision), and by examination of a cross-section. For the latter, the films were deposited on a thin silicon substrate in order to obtain a clear fracture of the substrate. The cross-sections were then examined with a Leitz Aristomet optical microscope (with a Leica DC 300 camera) and the thickness of the organic coatings deducted using the Leica Image Manager software.

2.4. Atomic force microscopy (AFM)

The Atomic Force Microscopy images and the average surface roughness measurements of the samples were obtained using an Autoprobe CP (Park Scientific Instrument) in non contact tapping mode. Two types of observations were performed: "Topographic Mode" observations where variations of colours on the picture obtained are due to differences of roughness and "Phase Mode" observations where these differences are due to difference in hardness of the material. All AFM measurements were performed in air at 25°C with a silicon nitride cantilever.

2.5. Electrochemical characterization

The electrochemical characterization was made using a traditional three-electrode electrochemical cell with a platinum wire as counter electrode and a saturated calomel electrode (SCE) as reference electrode. Figure 2. describes the electrochemical cell: the steel substrate is coated by the polymer on which is glued a PVC (Polyvinyl chloride) tube. The solution is then poured into the tube in which reference and counter electrodes are placed. The exposed area was 14 cm^2. The Electrochemical Impedance Spectroscopy tests were carried out in a 0.3% ($C = 2.1 \times 10^{-2}$ mol·L^{-1}) sodium sulphate solution at open circuit potential, with a 50 mV amplitude signal, a frequency range from 10^5 Hz to 1 Hz during the first 7 days of testing and 10^5 to 10^{-2} Hz for further measurements. All electrochemical experiments were performed with a frequency response analyser (Solartron 1260) connected to a potentiostat (Solartron 1287). Impedance diagrams were interpreted on the basis of equivalent circuits using Zview (Solartron Software). In order to perform accurate measurements, the electrochemical cell was placed in a Faraday cage.

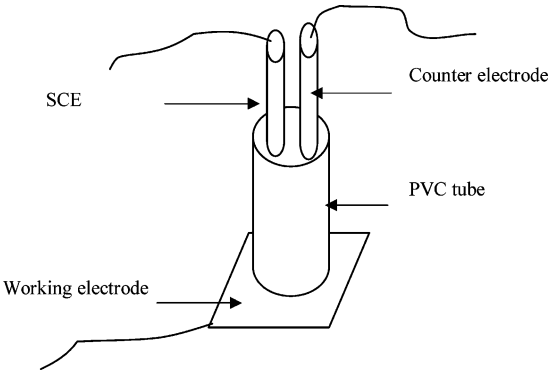

Fig. 2 Scheme of the electrochemical Cell

3. Results and discussion

3.1. Thickness of the coatings

The results obtained from the mass differences measurements and from the cross-section observations are reported in Table 4. The two methods give coherent values, about 50 μm for one layer even if the measures were difficult. Indeed, the dispersal of the optical measurements can be explained by the fact that the cross-section after fracture of the coated silicon substrate is not still evident (Fig. 3). Furthermore, the results obtained from mass difference measurements can be also slightly overestimated if the solvent did not completely evaporate.

3.2. Atomic force microscopy (AFM)

Samples 1.1, 1.3 and 1.6 were examined. The pictures obtained are very similar that is why only those corresponding to sample 1.1 are shown here. The Fig. 4(a). is a "Topographic

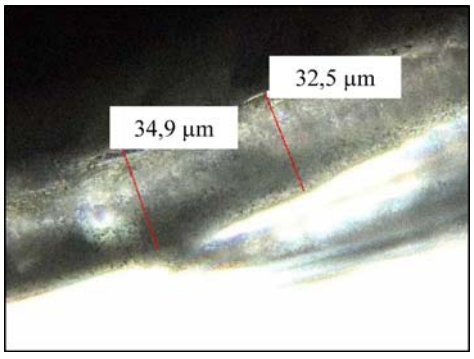

Fig. 3 Optical Microscope Observation of a Cross-Section

Mode" observation. On this image, one can observe that the 1.1 sample surface is relatively homogeneous with little roughness. Some small islands with a diameter of about 1 μm are distributed on the entire surface and are probably due to a bad evaporation of the solvent [12] which would cause defects leading to delamination of the film from the substrate. The roughness of the surface is about 10 nm. The Fig. 4(b) was obtained in "Phase Mode". This type of mode allows to differentiate soft phases and hard phases. So, the black small strips are characteristic of a "soft" phase identified as being the PBA block which has a low glassy transition temperature. On the other hand the white small strips correspond to "hard" phases: the PTFEMA block which has an high glassy transition temperature. So these phases arrangement pointed out the lamellar structure of the copolymer.

3.3. Electrochemical impedance

We present only diagrams of the diblock copolymers 1.1 and 1.6, which have the most remarkable behaviour, the copolymer 1.3 has an intermediate behaviour and copolymers 2.1 and 3.1 are less interesting from the point of view of corrosion resistance. On Fig. 5(a)–(c) are represented the diagrams in Nyquist representation of sample 1.1 obtained versus immersion time. On Fig. 6, the same diagrams are given in Bode-Modulus representation and on Fig. 7 diagrams of sample 1.6 versus immersion time.

On Fig. 5(a)–(c), for sample 1.1, three types of behaviour are recognizable:

(1) a capacitive behaviour until 12 hours of immersion (Fig. 5(a)). The coating is not affected by corrosion and can be modelled by an equivalent circuit with the resistance of the electrolyte (R_1) in series with the organic coating capacitance (CPE1) (Fig. 8(a)). This last element is in fact a constant phase element $C = CPE.\omega^{(n-1)}$. The fitting of experimental data gives a capacity of $7.9 \times 10^{-11}\,F \cdot cm^{-2}$ which is characteristic of an organic coating.
(2) After 24 hours of immersion, a time constant appears at high frequencies indicating the penetration of water in the coating (Fig. 5(b)). These diagrams can be explained by the equivalent circuit presented on Fig. 8(b). It is composed of the electrolyte resistance R_1, followed by a coating capacitance (CPE1) in parallel with a coating resistance (R_2). In this case, the coating is still little affected by corrosion.
(3) After two weeks of immersion, the first semi-circle contains, in fact, two time constants (Fig. 5(c)) at low frequencies due to the electrochemical contribution of steel through the defects of the coating. The first two behaviours indicate that the coating is enough waterproof or little affected by corrosion. When the second time constant appears, the substrate is exposed to the electrolyte and the coating is not anymore protective. The circuit of Fig. 8(c) is then used. However the water uptake results, which will be commented further, lead us to think, also, that it is not a question only of defects in the coating but also of a phenomenon of delamination.

On Fig. 6 are presented the same diagrams in Bode representation. The degradation of the coating after two weeks of

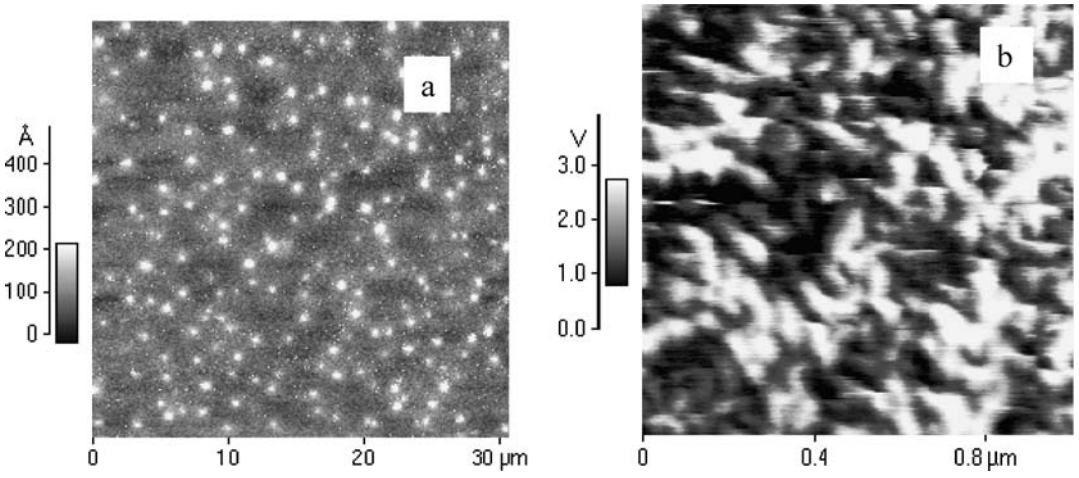

Fig. 4 (a) "Topographic Mode" Atomic Force Microscopy observations (30 μm). (b) "Phase Mode" Atomic Force Microscopy observations (1 μm)

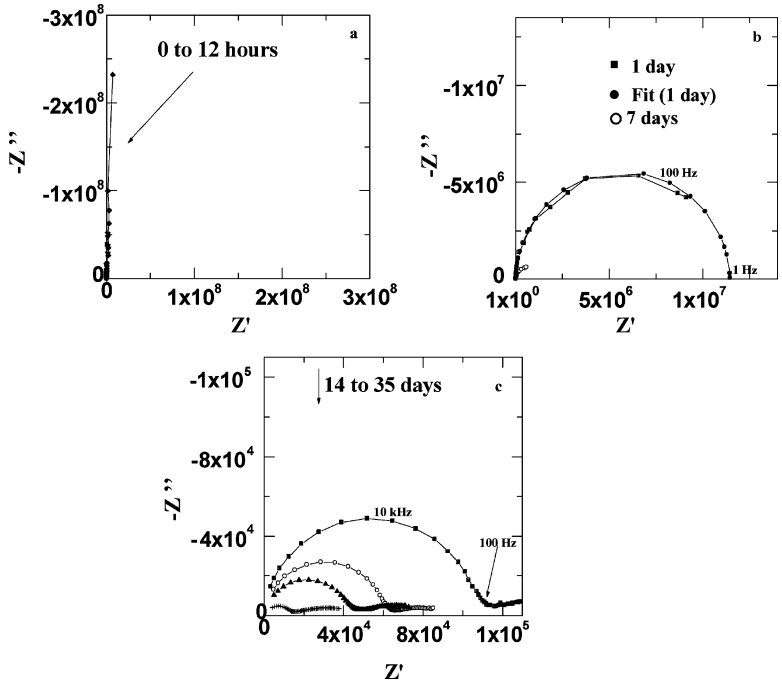

Fig. 5 Evolution of the impedance diagrams (in Nyquist representation) versus immersion time in a Na_2SO_4 (3 g/l) solution for sample 1.1: (a) Initial time, (b) From 1 to 7 days, (c) After 14 days

immersion is clearly distinguishable: indeed, the impedance modulus at low frequencies is then of the order of $10^6\ \Omega \cdot cm^2$ which is often considered as the threshold of acceptable protection for an organic coating.

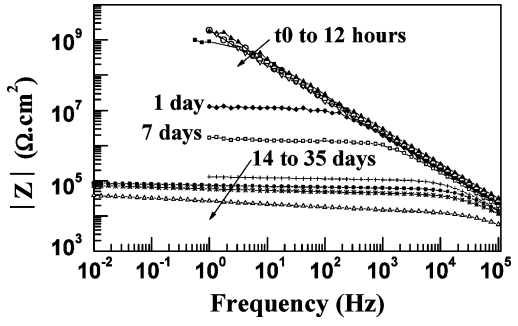

Fig. 6 Evolution of the impedance diagrams (Bode-Modulus representation) versus immersion time in Na_2SO_4 (3 g/l) solution for sample 1.1

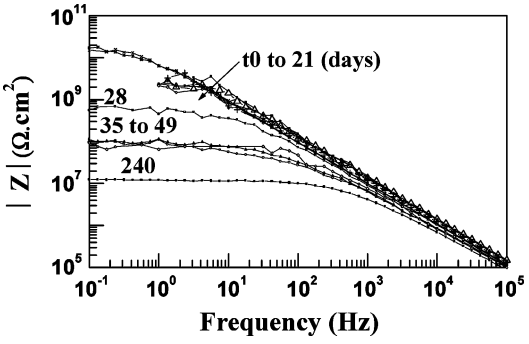

Fig. 7 Evolution of the impedance diagrams (Bode-Modulus representation) versus immersion time in a Na_2SO_4 (3 g/l) solution for sample 1.6

On Fig. 7 sample 1.6 shows initially impedance modulus values between 10^9 and $10^{10}\ \Omega \cdot cm^2$, values already higher than those of sample 1.1. Moreover even after eight months of immersion a good protective character is preserved. This confirms the essential role of the coating thickness.

Figure 9 summarises the evolution of the impedance modulus at 10 mHz according to the immersion time for all samples. The impedance modulus at low frequencies is an indication of the global corrosion resistance of the sample. The uncoated steel presents a characteristic low impedance modulus (around $10^4\ \Omega \cdot cm^2$). Sample 3.1 is very protective

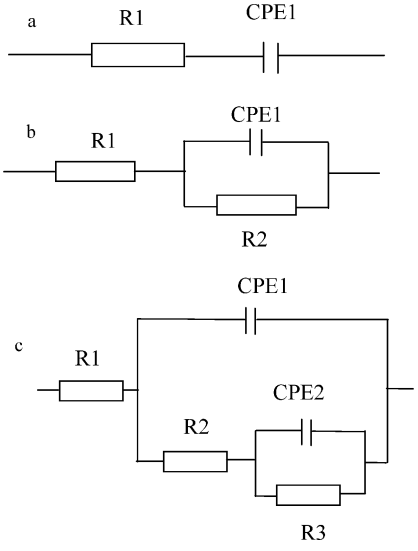

Fig. 8 Equivalent electrical circuits used for (a) a capacitive behaviour, (b) one time constant at high frequencies, (c) two time constants

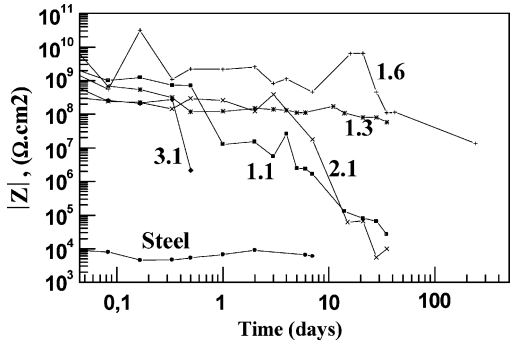

Fig. 9 Evolution of the impedance modulus at 10 mHz versus immersion time in a Na_2SO_4 (3 g/l) solution for each samples

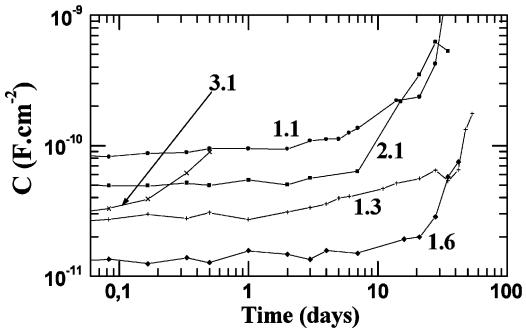

Fig. 10 Coating capacitance evolution versus immersion time in Na_2SO_4 3 g/l solution

initially but after only 12 hours the impedance modulus decreases drastically from 4.5×10^8 to $2 \times 10^6\ \Omega \cdot cm^2$. In the same way, the samples 1.1 and 2.1 are protective initially but undergo a slower degradation (a factor of 10 is observed) than sample 3.1. This could be explained by the nature of the nanostructuration. For the sample 3.1, a PTFEMA sphere nanostructuration in a PBA matrix [6] is expected whereas for samples 1.1 and 2.1 a lamellae nanostructuration was expected and observed by AFM (Section 3.2). Samples 1.3.a and 1.3.b present high values, even if initially these values are lower than the coatings having an uni-layer. Finally, the sample 1.6 presents an excellent protective behaviour even after 7 weeks of immersion. The impedance modulus values are between 10^8 and $10^9\ \Omega \cdot cm^2$. The comparison shows that use of dichloromethane as solvent as well as high PBA molar mass gives less interesting results. The expected contribution of thickness for corrosion protection is shown.

3.4. Capacitances of organic coatings

For characterising the protective properties of organic coatings, the coating capacitance is one of the most frequently studied parameters obtained by EIS measurements, it allows also to estimate the water uptake (Section 3.5).

From fitting of the data using the equivalent circuits described above, coating capacitances were deduced and plotted versus immersion time on Fig. 10. On this figure all capacitances are included between 10^{-11} and $10^{-10}\ F \cdot cm^{-2}$ and are characteristic of an organic coating. As in the case of impedance modulus evolution, the influence of the thickness is present. Indeed, for films having 3 and 6 layers, the obtained capacitances are respectively divided by 3 and 6. This is in agreement with the well-known formula which expresses the thickness dependence of capacitance:

$$C = \frac{\varepsilon \varepsilon_0 A}{d} \tag{1}$$

where ε is the dielectric constant of the coating, ε_o the dielectric permittivity of vacuum, A the sample area and d the coating thickness. In this equation, the coating capacitance is considered proportional to the dielectric constant, because the geometrical parameters are considered constant, like the coating thickness. But this assumption is not always true. The water uptake can cause swelling in the polymeric matrix of the coating. When the immersion time is increased, the capacitance increases too (for all coatings) due to the water penetration in the coating increasing the permittivity. For samples 1.1, 2.1, 3.1, we can observe a drastic increase of C, which can allow us to give same conclusions that in the part 3.3.

3.5. Water uptake

The determination of the volume fraction of water in organic coatings is often made by electrochemical impedance spectroscopy based upon the evolution of the coating capacitance, according to the Brasher - Kingsbury [13] equation (Eq. (2)).

$$\phi = \frac{100 \log(C_t / C_0)}{\log\ \varepsilon} \tag{2}$$

where C_t is the coating capacitance at time t, C_0 the capacitance of the dry coating, (usually obtained by extrapolation to the instant of immersion) and ε the dielectric constant of water.

The volume fraction was only calculated for the copolymer 1.1 and is reported on Fig. 11. These values are coherent with those given in the literature, i.e. between 4 and 6 percent of water absorbed after 2 days of immersion. We also found the general evolution for an organic coating: a diffusion of the electrolyte during the first day of immersion, following by a saturation phase during two days. After two days of immersion, the water uptake increases drastically indicating the deterioration of the coating (delamination). This phenomenon was not observed for the sample 1.6.

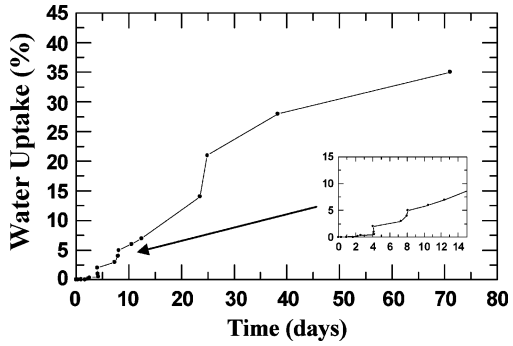

Fig. 11 Volume fraction versus immersion time in Na_2SO_4 3 g/l solution for sample 1.1

4. Conclusions

Poly(*n*-butyl acrylate-*b*-trifluoroethyl methacrylate) block copolymers were synthesised by Controlled Radical Polymerisation to achieve lamellae nanotructured organization on steel substrate. The thickness of the coatings (from 35 to 265 m) was determined by two different techniques: double weighing and optical microscopic observation of the cross-section of the coating on a thin silicon substrate. These two methods are in excellent agreement. The AFM observations showed a relatively homogeneous and slightly rough structure of the substrates. Electrochemical impedance spectroscopy shows that the use of dichloromethane as solvent is unfavourable. The same conclusion was obtained for the block copolymer with high PBA molar mass leading to a PTFEMA sphere nanostructured in a matrix of PBA: this result confirms the interest of lamellae nanostructured organization compare to the others. Indeed, their corrosion resistance quickly decreases after a few days (10) of immersion due to poor mechanical/adhesion properties of the coating ("sticky" surface). The impedance diagrams and in particular the comparison of the impedance modulus at low frequency for each samples versus immersion time showed logically that an increase of thickness improved the waterproof character of the coating. The thickest coating (sample 1.6) always presents a very good corrosion resistance even after eight months of immersion.

Other tests (in more aggressive solution such as NaCl) and other block copolymer types will be studied in order to optimize the corrosion resistance and the adhesion to the substrate for lower the thickness.

Acknowledgments The authors thank the Deutsch-Französische Hochschule that supported the "First German-French Summer School on Electrochemistry and Nanotechnology" as well as the University of Erlangen-Nuremberg, University of Provence, CNRS, Metrohm, Autolab, Raith for their financial contributions and Arkema for MAMA-SG1 and SG1 products.

References

1. Determination of coating performance with impedance measurements, TNO Centre for Coatings Research Delft, The Netherlands, (1992).
2. N.S. Sangaj and V.C. Malshe, *Progress in Organic Coatings*, **50**, 28 (2004).
3. C.M. Hansen, *Progress in Organic Coatings*, **51**, 55 (2004).
4. C. K. Schoff, *Progress in Organic Coatings,* (2004).
5. L.H. Sperling, *Introduction to Physical Polymer Science*, 2nd Edition, J. Wiley & Sons, (1992), Chapter 4.
6. I.W. Hamley, *The Physics of Block Copolymers*, ed. Oxford Science Publications, (1998), Chapter 2.
7. D. Bertin, M. Destarac, B. Boutevin, *Polymers and Surfaces*, **47** (1998).
8. P.L. Bonora, F. Deflorian, and L. Fedrizzi, *Electrochimica Acta*, **41**, 1073 (1996).
9. F. Deflorian, L. Fedrizzi, S. Rossi, and P.L. Bonora, *Electrochimica Acta*, **44**, 4243 (1999).
10. Z. Kloek, *Progress in Organic Coatings*, **30**, 287 (1997).
11. F. Deflorian, L. Fedrizzi, S. Rossi, F. Buratti, and P.L. Bonora, *Progress in Organic Coatings*, **39**, 9 (2000).
12. T. To, H. Wang, A.B. Djurisic, M.H. Xie, W.K. Chan, Z. Xie, C. Wu, S.Y. Tong, *Thin Solid Films*, **467**, 59 (2004).
13. D.M. Brasher and A.H. Kingsbury, *J. Appl. Chem*., **4**, 62 (1954).